

## Research Article

# Inulin-Grafted Stearate (In-g-St) as the Effective Self-Assembling Polymeric Micelle: Synthesis and Evaluation for the Delivery of Betamethasone

Gholamabbas Chehardoli,<sup>1</sup> Parham Norouzian,<sup>2</sup> and Farzin Firozian <sup>2</sup>

<sup>1</sup>Medicinal Plants and Natural Products Research Center, Hamadan University of Medical Sciences, Hamadan, Iran

<sup>2</sup>Department of Pharmaceutics, School of Pharmacy, Hamadan University of Medical Sciences, Hamadan, Iran

Correspondence should be addressed to Farzin Firozian; [ffirozian@yahoo.com](mailto:ffirozian@yahoo.com)

Received 22 February 2020; Accepted 15 April 2020; Published 26 May 2020

Academic Editor: Ruibing Wang

Copyright © 2020 Gholamabbas Chehardoli et al. This is an open access article distributed under the Creative Commons Attribution License, which permits unrestricted use, distribution, and reproduction in any medium, provided the original work is properly cited.

**Background.** Betamethasone as a corticosteroid drug is commonly used for the treatment of rheumatoid arthritis. Unfortunately, betamethasone is a low water-soluble drug and its efficacy is low. So an attractive strategy is the targeted delivery of betamethasone to the damaged joint using polymeric micelle-based carriers. **Methods.** Inulin-grafted stearate (In-g-St) was synthesized via the reaction of stearoyl chloride and inulin, then characterized by FT-IR and H-NMR. In-g-St forms micelles in the presence of betamethasone. The prepared polymeric micelles were characterized for size, zeta potential, drug loading, particles' morphology, critical micelle concentration (CMC), and encapsulation efficiency. So sustained release polymeric micelles of betamethasone were developed by employing In-g-St. **Results.** The measurement of particle size showed a mean diameter of 60 and 130 nm for 10% and 20% drug-loaded micelles, respectively, and SEM showed that the particle's morphologies are spherical. Zeta potential measurement for the drug-containing micelles showed a value of -11.8 mV. Drug loading efficiency and the encapsulation efficiency were 6.36% and 63.6%, as well as 18.97% and 94.88% for 10% and 20%, respectively. 20% drug-loaded polymer showed a small burst release of betamethasone at the first 3 h which was followed by sustained release in the next 24 h. Furthermore, the formula with 10% exhibited good sustained release properties except for the minor initial burst release. **Conclusion.** Data from the zeta potential, CMC, drug loading capacity, and in vitro drug release studies indicated that In-g-St polymeric micelles can be suitable candidates for the efficient delivery of hydrophobic drugs like betamethasone.

## 1. Introduction

Rheumatoid arthritis (RA), as one of the autoimmune and chronic inflammatory diseases, has affected approximately 1% of the world's population [1]. This disease arises more commonly in the elderly people primarily determined by the pain and swelling in the small joints and wrist of the hands and feet, which in severe cases can lead to the progressive disability and premature death [2]. Currently, early diagnosis and treatment strategies that are based on glucocorticoids and nonsteroidal anti-inflammatory drugs could improve the RA patient's quality of life [3]. Glucocorticoids or corticosteroids such as prednisone prednisolone, dexamethasone, and betamethasone as synthetic compounds similar to cortisol hormone can help to reduce the inflammation, stiffness, and pain of the swollen joints [4]. While there is currently no promising cure for RA, different pharmacologic therapy strategies are aimed at increasing the efficacy of existing drugs and attenuating disease progression and decrease and/or delay deformity of joints [5]. Therefore, even though long-term disease remission is not yet achieved for many patients and also the increasing number of various drugs and treatment regimes, novel strategies for drug delivery and new therapeutic options are required [5, 6].

Betamethasone as one of the effective synthetic corticosteroid drugs is commonly used for the treatment of RA by

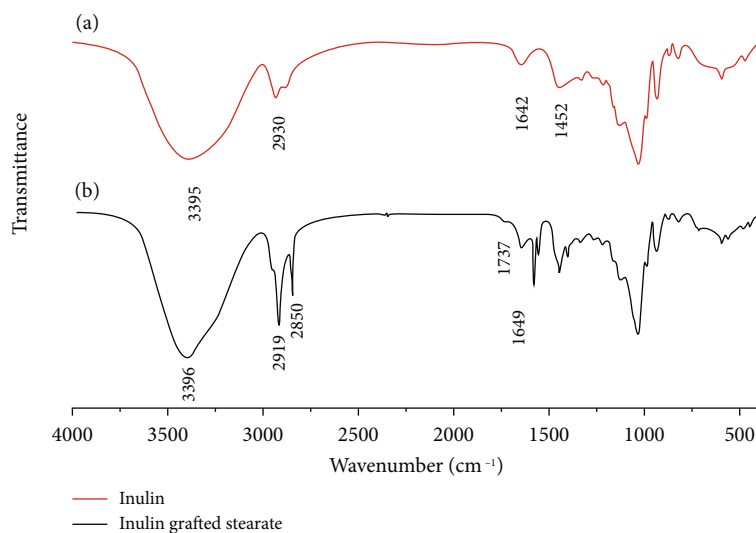


FIGURE 1: The FT-IR spectrum of inulin (a) and inulin-grafted stearate (b).

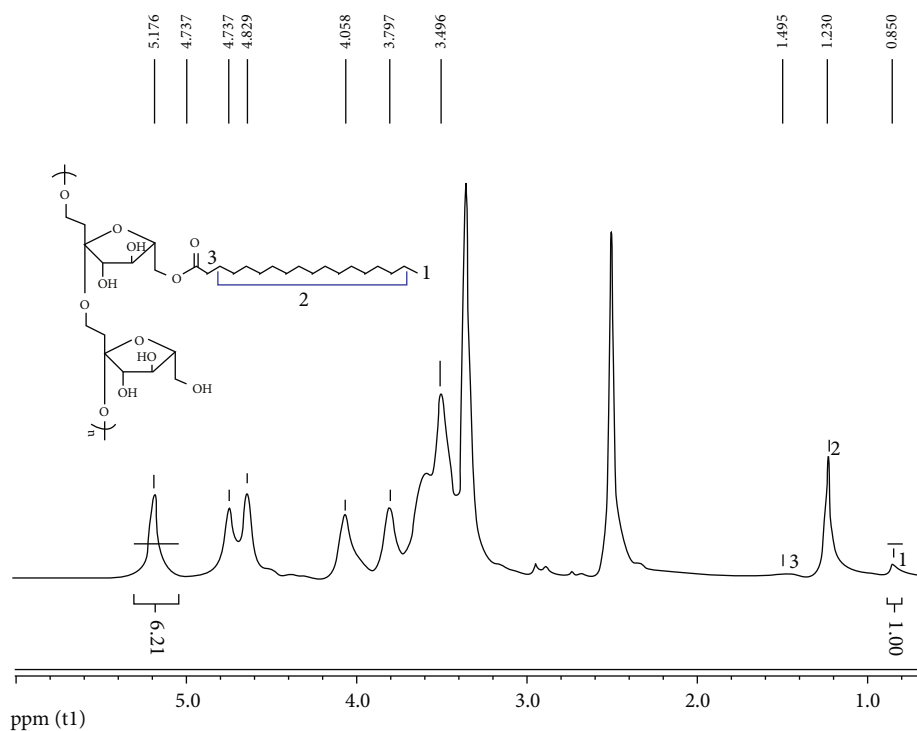


FIGURE 2: <sup>1</sup>H-NMR spectrum of the In-g-St in DMSO-d<sub>6</sub>.

attenuating inflammation and slowing joint damage [7]. However, these kinds of drugs also face some limitations, of which the most important ones are their toxicity especially with long-term use, low solubility, frequent administrations, and side effects on other tissues [8]. To overcome these problems, some strategies were introduced such as reducing toxicity by intra-articular administration of the drug and minimizing exposure of the drug to other tissues, but in RA, this requires repeated joint needling into a large number of joints, which faces treatment with other complications [9].

Therefore, an attractive strategy is the targeted delivery of betamethasone to the damaged joint using liposomes and polymeric micelle-based carriers. Over recent decades, there has been considerable interest in liposomes, polymeric micelles, and other nanoparticles as pharmaceutical nanocarriers for encapsulating various drugs and an effective option for their delivery to the target tissue [10–14]. In this regard, liposome-encapsulated betamethasone has been proven to be very effective for increasing the uptake and stability of the drug in the synovial cavity of damaged joints

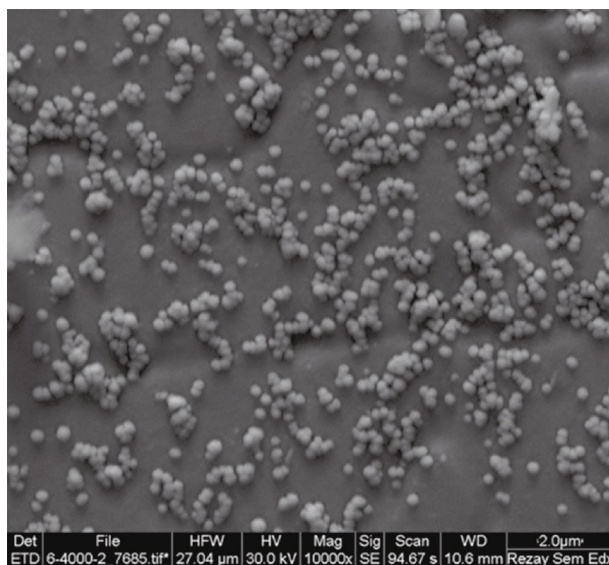


FIGURE 3: SEM micrograph of betamethasone-loaded polymeric micelle.

TABLE 1: Physical characteristics of In-g-St polymeric micelles.

Formulation	Size (nm)	DL% (w/w)	EE% (w/w)	Zeta potential (mv)
10% formula	127.1 ± 5.6	6.36% ± 0.02	63.6% ± 0.22	-12.7 ± 0.9
20% formula	57.5 ± 2.6	18.50% ± 0.58	94.89% ± 2.91	-13.4 ± 4.2

[15–17]. Besides liposomes, polymer micelles as drug carriers can also be targeted at the damaged site [18, 19]. The advantage of these nanoparticles is their low leakage, light stability, cheap industrial production, and their ease of use compared to liposomes [5, 20]. Besides, by formulating insoluble drugs in the form of lyophilized polymeric micelles, it can be considered as an injectable and stable dosage form candidate for the treatment of the condition by the medical community [14].

Inulin, which is found as a group of natural polysaccharides [21–23] in various plants, with hydrophobic groups can form polymeric micelles in the aqueous solutions. Unique physicochemical properties (nontoxicity, biocompatibility, and water solubility), low-cost production, and their efficiency have introduced inulin as the attractive starting material to develop new drug carriers [24–27].

In continuation of our studies on the polymer manipulation [28] specially grafting [29], in the present study, inulin-grafted stearate (In-g-St) would be synthesized for the formation of polymeric micelles as suitable carriers of betamethasone. Also, the release profile of betamethasone from the polymeric micelles has been studied.

## 2. Material and Methods

### 2.1. Synthesis of Inulin-Grafted Stearate Polymeric Micelles.

Under the  $N_2$  atmosphere, 2 g of inulin was mixed with 4 g lithium chloride in 20 mL of dimethylformamide

(DMF) at 120°C. The mixture was stirred while reaching a clear and colorless solution. After decreasing the temperature to 80°C, 360 mg dimethylaminopyridine and 840  $\mu$ L stearoyl chloride were added to the solution and refluxed for 24 hours. Then, the reaction mixture was dialyzed in 1 L ethanol by dialysis tubing with cutoff 2000 Da. After 12 hours, the dialysis tubing was transferred to 1 L water and the proses were continued up to 24 hours. Ultimately, by freeze-drying of the final solution, the lyophilized modified polymer was achieved.

**2.2. Critical Micelle Concentration (CMC) Assay.** The critical micelle concentration (CMC) of the In-g-St polymer was determined by studying the fluorescence spectra of pyrene as a hydrophobic fluorescent probe. Using the phosphate-buffered solution (PBS, pH = 7.4), the different concentrations of polymer solutions from 1.55  $\mu$ g/mL to 200  $\mu$ g/mL were prepared and then mixed with 1 mL of pyrene solution  $6 \times 10^{-6}$  mol/L in acetone while being stirred overnight to give the final concentration of pyrene ( $6 \times 10^{-7}$  mol/L).

The fluorescence emission spectra of the solutions and pure pyrene solution in the PBS were obtained at a fixed emission wavelength ( $\lambda_{em}$ ) of 390 nm. Based on the survey done on these spectrum fluorescence intensities of the samples at  $\lambda_{ex}$  = 335 nm and 338 nm as determined using a fluorescence spectrophotometer, FP-6000.

The changes in the ratio of fluorescence intensity  $\lambda_{ex}$  = 338 nm to 335 nm ( $I_{335}/I_{337}$ ) of pyrene were plotted against

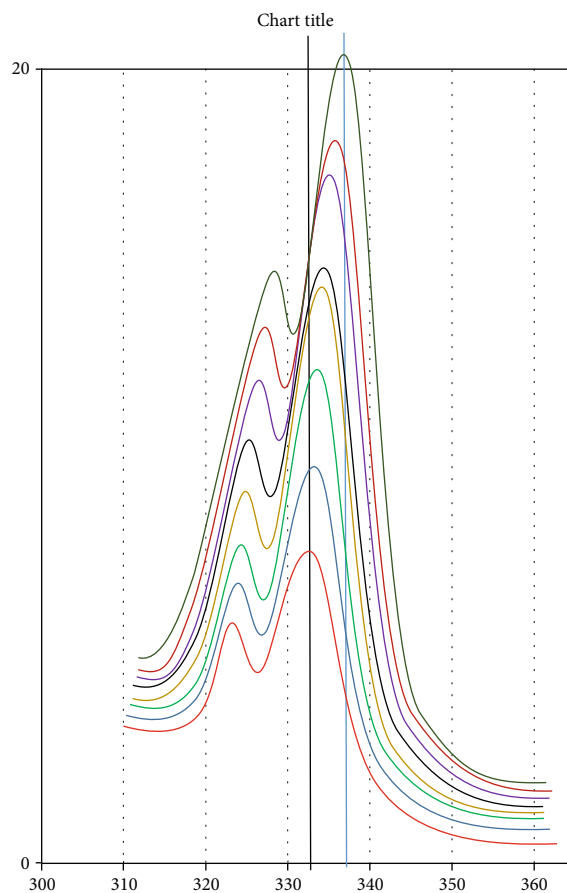


FIGURE 4: Fluorescence emission spectra of pyrene in the presence of decreasing concentrations of In-g-St at pH 7.4.

the log concentration of the In-g-St polymer for finding the CMC.

**2.3. Loading of Betamethasone onto Polymeric Micelles and Drug Loading Efficiency.** A dialysis method was used for the preparation of betamethasone-loaded micelles (10% and 20%). Briefly, 20 and 40 mg of betamethasone were added to 160 and 180 mg of (In-g-St), respectively, and the mixture was dissolved in 5 mL dimethyl sulfoxide (DMSO) and stirred for 1 hour at room temperature. To remove the unloaded drug and DMSO, the mixture was poured into a dialysis tube (Molecular cut off 2000 Da) and dialyzed against 1 L water for 1 hour; then, the dialysis solution was exchanged with the same amount of freshwater and the press was continued up to 24 hours. Thereafter, by freeze-drying, the lyophilized powder was obtained. In order to determine the percentage of betamethasone encapsulated in nanoparticles, a high-performance liquid chromatography (HPLC) analysis method was used. Briefly, 4 mg of each drug-loaded polymer (10% and 20%) dissolved in 10 mL DMSO; then, 1 mL of this solution was mixed with acetonitrile to make 10 mL volume of the final solution. After that, betamethasone concentration was determined by HPLC with ultraviolet detection at 240 nm using a Shimadzu apparatus (Shimadzu

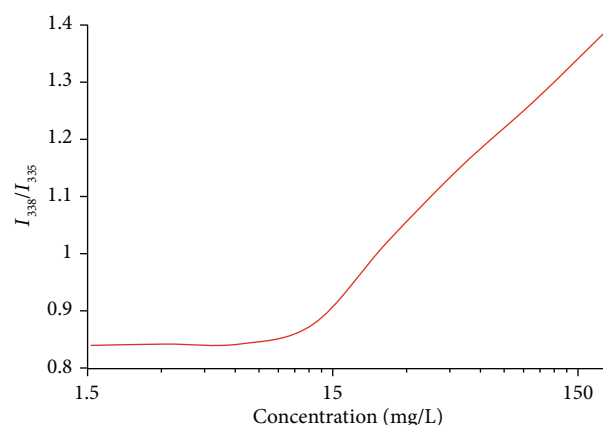


FIGURE 5: Plot for calculation of CMC of In-g-St using pyrene as the fluorescent probe.

Corp., Model LC-20AD XR, Japan) equipped with an auto-sampler. Betamethasone loading efficiency (%) and loading content (%) of the prepared formulation were calculated as follows:

$$\begin{aligned} \text{Encapsulation efficiency (EE) (\%)} &= \frac{\text{Mass of betamethasone within the nanoparticle}}{\text{Mass of betamethasone initially used}} \times 100, \\ \text{Drug loading (DL) (\%)} &= \frac{\text{Mass of betamethasone within the nanoparticle}}{\text{Mass of nanoparticle}} \times 100. \end{aligned} \quad (1)$$

**2.4. Particle Size Distribution Measurements.** Particle size, surface charge, and particle size distribution of betamethasone-loaded In-g-St nanoparticles were determined using a nanosizer apparatus (Nano-ZS; Malvern Instruments, United Kingdom).

One mL of betamethasone-loaded micelle was diluted in deionized water, and the micelle size was determined by Zetasizer Nano ZS instrument at a wavelength of 633 nm at 25°C with a detection angle of 90°.

**2.5. Characterization of Particle Morphology.** Transmission electron microscopy (TEM) and scanning electron microscopy (SEM) techniques are used to evaluate the morphology of nanoparticles [30–33]. In this study, we used the SEM technique. SEM assay is performed at the central laboratory of Shahid Chamran University of Ahvaz by using a scanning electron microscope apparatus (Model 1455 VP manufactured by DME).

**2.6. In Vitro Drug Release Evaluation.** The evaluation of betamethasone release profile from micelle formulation was performed by the dialysis method. In brief, 25 mg of betamethasone-loaded micelle powder was dispersed in 2 mL of phosphate-buffered saline (pH 7.4), then added into the dialysis tubes (cut off 12000 Da). The tube was placed in a 100 mL bottle of phosphate-buffered saline (pH 7.4). Then,

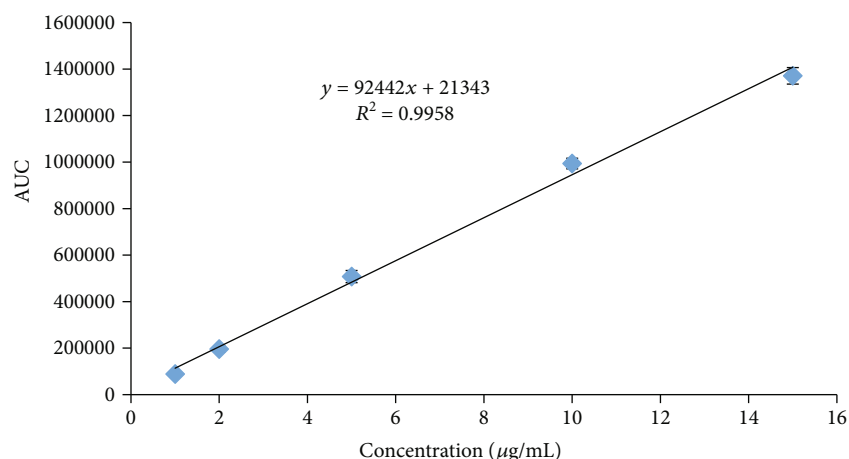


FIGURE 6: Calibration curve of betamethasone.

the capped bottles were incubated at 150 RPM spinning in 37°C shaker incubator. The samples were withdrawn at 1, 3, 6, 12, and 24 hours; then, the concentration of the drug in the samples was evaluated by the HPLC method.

### 3. Results and Discussion

#### 3.1. Characterization of the Synthesized Polymer (In-g-St)

**3.1.1. FT-IR Study.** The FT-IR spectra of inulin (a) and inulin-grafted stearate (b) are presented in Figure 1. The strong and broad-band peak between 3000 and 3600  $\text{cm}^{-1}$  was assigned to O–H stretching vibrations. Two peaks which appeared in 2919 and 2850  $\text{cm}^{-1}$  indicate the stretching vibrations of aliphatic C–H of the stearate group. Compared to the inulin spectrum, a new weak band in 1737  $\text{cm}^{-1}$  (highlighted as a green curve) was assigned to the carbonyl group of an ester, which confirmed the grafting of the stearate group to the inulin via an esterification reaction. While only a few monomers of the polysaccharide are substituted with stearate groups, the esoteric peak is seen as a shoulder. This phenomenon has been observed in previous studies that have been conducted at the chemical modification of polysaccharides [29, 34–36].

**3.1.2.  $^1\text{H}$ -NMR Study.** Another confirmation of the grafting reaction is the  $^1\text{H}$ -NMR spectrum of the In-g-St (Figure 2). The absorption peak at  $\delta = 0.850$  ppm was assigned to the terminal methyl group of the stearate. Methylene groups of the St appeared in  $\delta = 1.230$  and 1.495 ppm. The region of the stearate peaks in our polymer is consistent with the reported paper [36]. The peaks appear in regions 3.495, 3.797, 4.058, 4.629, 4.737, and 5.176 related to the inulin backbone [37].

**3.1.3. Degree of Substitution.** Degree of substitution of In-g-St was achieved in the manner reported by Mandracchia et al. [26]. It was calculated as the ratio between the integral of the peak at 0.85 ppm belonging to the terminal methyl group of the stearate and the integral of the peak at 5.176 ppm

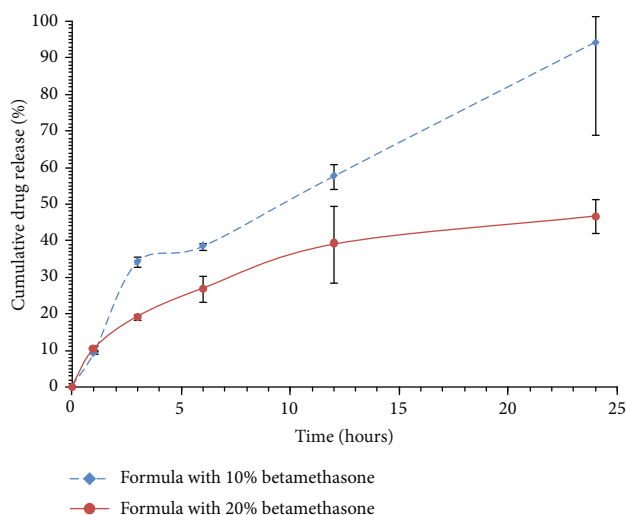


FIGURE 7: In vitro betamethasone release from betamethasone-loaded In-g-St micelles for two formulations.

belonging to the anomeric proton of fructose unit of inulin [37]. The degree of substitution is 16.1%.

#### 3.2. Characterization of Betamethasone-Loaded Polymeric Micelles

**3.2.1. Scanning Electron Microscopy (SEM).** Polymeric micelles comprise a hydrophobic core enclosed by a hydrophilic shell, and they are generally synthesized from an amphiphilic copolymer with self-assembling properties in water. This structure causes reducing systemic side-effects and improving therapeutic efficiency, especially for poorly soluble drugs such as betamethasone [20].

The morphology of the micelles is determined by SEM. SEM micrograph of micelles containing betamethasone-loaded In-g-St shows the round homogeneously dispersed particles with a regular spherical shape (Figure 3) which is an important factor for articular delivery [38]. Regarding the homogenous spherical shape of In-g-St particles, in a study by Mandracchia et al. [26], SEM pictures also



represented homogeneously dispersed round particles of inulin-based micelle loaded with hydrophobic drugs.

**3.2.2. Zeta Potential.** Zeta potential is commonly used to determine the surface charge of NPs and is an important factor that directly affects the stability of NPs [39]. Zeta potential for betamethasone-loaded In-g-St was measured which showed the surface charge of  $-13.4$  mV. This negative charge is due to the presence of stearate moieties in inulin structure which is present on the surface of the NPs [40]. Though the surface charge is negative to some extent, betamethasone-loaded In-g-St NPs have enough repulsive force to prevent aggregation during long-term storage [41, 42]. In accordance with our results, Kim et al. have shown negative results for zeta potential of phthalyl inulin NPs ranged from  $-21.29$  to  $-27.91$  mV [43]. The very small size and the negative surface charges allow this system to pass through the cell membranes.

**3.2.3. Encapsulation Efficiency (EE) and Drug Loading (DL) Capacity.** The high encapsulation efficiency is owing to high affinity of drug and the modified polymer in the same media (organic or aqueous phase) [44]. Encapsulation efficiency and drug loading of the betamethasone-loaded In-g-St NPs were found to be 63.38% and 6.36% for 10% polymer and 92.54% and 18.50%, for 20% polymer, respectively (Table 1).

The In-g-St nanoparticles in comparison with dextran stearate polymeric micelles show that the inulin-derived particle was significantly smaller, which could be due to the lack of branching in the In-g-St polymer. In addition, it is much easier and less costly to produce low molecular weight of inulin than other polysaccharides [34, 35].

**3.2.4. CMC of In-g-St Polymer.** CMC is defined as the minimum polymer concentration required for the micelle formation; therefore, it is an important parameter for the characterization of micelle stability. The lower CMC values cause the more thermodynamic stability of the polymeric micelles [45].

The CMC of the In-g-St was evaluated via a shift of the intensity ratio of the pyrene fluorescence bands due to the passage of the hydrophobic pyrene from a hydrophilic to a hydrophobic environment. The ratio of fluorescence intensity of the third energy in  $\lambda_{\text{ex}} = 338$  nm ( $I_{338}$ ) which is higher in the molecule placed in the hydrophobic microenvironment and  $\lambda_{\text{ex}} = 335$  nm which is higher in the polar environment can be used as the index of the polarity of its microenvironment (Figure 4).

The CMC was determined from the intersection of the straight line and the horizontal lines at the low and high concentration ranges, respectively, which was  $6.2 \mu\text{g/mL}$  (Figure 5). Therefore, In-g-St copolymers can form a more thermodynamically stable micelle under high-dilution conditions.

**3.2.5. In Vitro Drug Release.** In order to determine the drug release behaviors of drug-loaded In-g-St polymer, release experiments were performed in phosphate buffered saline (PBS, pH = 7.4) by HPLC analysis technique. The calibration curve and plot of % cumulative drug release are rep-

resented in Figures 6 and 7. As seen in Figure 7, 20% drug-loaded polymer showed a small burst release of betamethasone at the first 3 h of the experiment which was followed by sustain release in the next 24 h. The burst release is related to the more concentrations of drug molecules which were presented in the surfaces of the micelles. Furthermore, the formula with 10% drug exhibited good sustained release properties except for the minor initial burst release. The sustained release of betamethasone from In-g-St micelle is the result of interaction between these hydrophobic drug molecules and the lipophilic core of the micelles that acts as a reservoir of the drug which released drug molecules slowly. In the literature, similar inulin-based drug delivery systems show similar release behaviors. For example, Mandracchia et al. have shown the sustained and sensitive release of celecoxib from inulin-d-alpha-tocopherol succinate (INVITE) nanomicelles [46].

## 4. Conclusion

In this study, we synthesized a novel derivative of inulin via the reaction of stearyl chloride and inulin. FT-IR and H-NMR spectra confirmed the formation of the modified polysaccharide. Drug loading studies, particle size analysis, and the images of the electron microscope showed that betamethasone was efficiently loaded onto the modified polysaccharide and the micelles were formed successfully. The modified polymer low CMC level indicated that the micelles have acceptable stability. In-g-St polymeric micelles could be the suitable candidates to the controlled release of the lipophilic drugs such as betamethasone. In-g-St has two major advantages over dextran-g-St: first, it is cheaper, and second, it forms smaller micelles.

## Abbreviations

In-g-St:	Inulin-grafted stearate
CMC:	Critical micelle concentration
SEM:	Scanning electron microscopy
RA:	Rheumatoid arthritis
DMF:	Dimethylformamide
DMSO:	Dimethyl sulfoxide
EE:	Encapsulation efficiency
DL:	Drug loading
PBS:	Phosphate-buffered solution
NPs:	Nanoparticles.

## Data Availability

The data used to support the findings of this study are available from the corresponding author upon request.

## Conflicts of Interest

Authors declare that they have no conflict of interest.

## Acknowledgments

This work was financed by the Deputy of Research, Hamadan University of Medical Sciences (Grant number 9603091600).

## References

- [1] I. Rudan, S. Sidhu, A. Papana et al., "Prevalence of rheumatoid arthritis in low- and middle-income countries: a systematic review and analysis," *Journal of Global Health*, vol. 5, no. 1, 2015.
- [2] I. B. McInnes and G. Schett, "Pathogenetic insights from the treatment of rheumatoid arthritis," *The Lancet*, vol. 389, no. 10086, pp. 2328–2337, 2017.
- [3] G. R. Burmester and J. E. Pope, "Novel treatment strategies in rheumatoid arthritis," *The Lancet*, vol. 389, no. 10086, pp. 2338–2348, 2017.
- [4] A. Kavanaugh and A. F. Wells, "Benefits and risks of low-dose glucocorticoid treatment in the patient with rheumatoid arthritis," *Rheumatology*, vol. 53, no. 10, pp. 1742–1751, 2014.
- [5] M. Chen, K. A. Daddy, Y. Xiao, Q. Ping, and L. Zong, "Advanced nanomedicine for rheumatoid arthritis treatment: focus on active targeting," *Expert Opinion on Drug Delivery*, vol. 14, no. 10, pp. 1141–1144, 2017.
- [6] Q. Wang and X. Sun, "Recent advances in nanomedicines for the treatment of rheumatoid arthritis," *Biomaterials Science*, vol. 5, no. 8, pp. 1407–1420, 2017.
- [7] D. Dragos, M. Gilca, L. Gaman et al., "Phytomedicine in joint disorders," *Nutrients*, vol. 9, no. 1, p. 70, 2017.
- [8] N. Saki, S. Hosseinpour, A. Heiran, A. Mohammadi, and M. Zeraatpishe, "Comparing the efficacy of triamcinolone acetonide iontophoresis versus topical calcipotriol/betamethasone dipropionate in treating nail psoriasis: a bilateral controlled clinical trial," *Dermatology Research and Practice*, vol. 2018, Article ID 2637691, 7 pages, 2018.
- [9] H. K. Knych, S. D. Stanley, L. M. Harrison, and D. S. McKemie, "Pharmacokinetics of betamethasone in plasma, urine, and synovial fluid following intra-articular administration to exercised thoroughbred horses," *Drug Testing and Analysis*, vol. 9, no. 9, pp. 1385–1391, 2017.
- [10] N. H. Moghadam, S. Salehzadeh, J. Rakhshshah et al., "Improving antiproliferative effect of the nevirapine on Hela cells by loading onto chitosan coated magnetic nanoparticles as a fully biocompatible nano drug carrier," *International Journal of Biological Macromolecules*, vol. 118, Part A, pp. 1220–1228, 2018.
- [11] N. H. Moghadam, S. Salehzadeh, J. Rakhshshah, A. H. Moghadam, H. Tanzadehpahan, and M. Saidijam, "Preparation of a highly stable drug carrier by efficient immobilization of human serum albumin (HSA) on drug-loaded magnetic iron oxide nanoparticles," *International Journal of Biological Macromolecules*, vol. 125, pp. 931–940, 2019.
- [12] M. Yang, X. Feng, J. Ding, F. Chang, and X. Chen, "Nanotherapeutics relieve rheumatoid arthritis," *Journal of Controlled Release*, vol. 252, pp. 108–124, 2017.
- [13] Q. Wang, J. Jiang, W. Chen, H. Jiang, Z. Zhang, and X. Sun, "Targeted delivery of low-dose dexamethasone using PCL-PEG micelles for effective treatment of rheumatoid arthritis," *Journal of Controlled Release*, vol. 230, pp. 64–72, 2016.
- [14] L. K. Prasad, H. O'Mary, and Z. Cui, "Nanomedicine delivers promising treatments for rheumatoid arthritis," *Nanomedicine*, vol. 10, no. 13, pp. 2063–2074, 2015.
- [15] B. Kapoor, S. K. Singh, M. Gulati, R. Gupta, and Y. Vaidya, "Application of liposomes in treatment of rheumatoid arthritis: quo vadis," *The Scientific World Journal*, vol. 2014, Article ID 978351, 17 pages, 2014.
- [16] F. Wang, X. Bao, A. Fang et al., "Nanoliposome-encapsulated brinzolamide-hydropropyl- $\beta$ -cyclodextrin inclusion complex: a potential therapeutic ocular drug-delivery system," *Frontiers in Pharmacology*, vol. 9, p. 91, 2018.
- [17] Y. Zhang, X. Wu, H. Li, N. Du, S. Song, and W. Hou, "Preparation and characterization of (betamethasone sodium phosphate intercalated layered double hydroxide)@ liposome nanocomposites," *Colloids and Surfaces A: Physicochemical and Engineering Aspects*, vol. 529, pp. 824–831, 2017.
- [18] S. Md, J. K. A./, P. Kuldeep Singh, M. Waqas et al., "Nanoencapsulation of betamethasone valerate using high pressure homogenization-solvent evaporation technique: optimization of formulation and process parameters for efficient dermal targeting," *Drug Development and Industrial Pharmacy*, vol. 45, no. 2, pp. 323–332, 2018.
- [19] M. Lapteva, K. Mondon, M. Möller, R. Gurny, and Y. N. Kalia, "Polymeric micelle nanocarriers for the cutaneous delivery of tacrolimus: a targeted approach for the treatment of psoriasis," *Molecular Pharmaceutics*, vol. 11, no. 9, pp. 2989–3001, 2014.
- [20] S. Parveen, R. Misra, and S. K. Sahoo, "Nanoparticles: a boon to drug delivery, therapeutics, diagnostics and imaging," *Nanomedicine: Nanotechnology, Biology, and Medicine*, vol. 8, no. 2, pp. 147–166, 2012.
- [21] Y.-F. Ding, S. Li, L. Liang et al., "Highly biocompatible chlorin e6-loaded chitosan nanoparticles for improved photodynamic cancer therapy," *ACS Applied Materials & Interfaces*, vol. 10, no. 12, pp. 9980–9987, 2018.
- [22] Y.-F. Ding, J. Wei, S. Li, Y.-T. Pan, L.-H. Wang, and R. Wang, "Host-guest interactions initiated supramolecular chitosan nanogels for selective intracellular drug delivery," *ACS Applied Materials & Interfaces*, vol. 11, no. 32, pp. 28665–28670, 2019.
- [23] C. Gao, F. Tang, G. Gong et al., "pH-responsive prodrug nanoparticles based on a sodium alginate derivative for selective co-release of doxorubicin and curcumin into tumor cells," *Nanoscale*, vol. 9, no. 34, pp. 12533–12542, 2017.
- [24] H. B. Andersson, L. H. Ellegård, and I. G. Bosaeus, "Nondigestibility characteristics of inulin and oligofructose in humans," *The Journal of Nutrition*, vol. 129, no. 7, pp. 1428S–1430S, 1999.
- [25] G. Di Prima, S. Saladino, F. Bongiovì et al., "Novel inulin-based mucoadhesive micelles loaded with corticosteroids as potential transcorneal permeation enhancers," *European Journal of Pharmaceutics and Biopharmaceutics*, vol. 117, pp. 385–399, 2017.
- [26] D. Mandracchia, G. Tripodo, A. Trapani et al., "Inulin based micelles loaded with curcumin or celecoxib with effective anti-angiogenic activity," *European Journal of Pharmaceutical Sciences*, vol. 93, pp. 141–146, 2016.
- [27] D. Wang, F. Sun, C. Lu et al., "Inulin based glutathione-responsive delivery system for colon cancer treatment," *International Journal of Biological Macromolecules*, vol. 111, pp. 1264–1272, 2018.
- [28] M. A. Zolfigol, G. Chehardoli, and M. Shiri, "Epoxidation of aromatic  $\alpha$ ,  $\beta$ -unsaturated ketones using PVP-H<sub>2</sub>O<sub>2</sub> under mild and heterogeneous conditions," *Reactive and Functional Polymers*, vol. 67, no. 8, pp. 723–727, 2007.
- [29] G. Chehardoli, H. Bagheri, and F. Firozian, "Synthesis of sodium alginate grafted stearate acid (NaAlg-g-St) and evaluation of the polymer as drug release controlling matrix," *Journal of Polymer Research*, vol. 26, no. 7, p. 175, 2019.

- [30] E. E. Kaya, O. Kaya, G. Alkan, S. Gürmen, S. Stopic, and B. Friedrich, "New proposal for size and size-distribution evaluation of nanoparticles synthesized via ultrasonic spray pyrolysis using search algorithm based on image-processing technique," *Materials*, vol. 13, no. 1, p. 38, 2020.
- [31] S. Lu, W. Ma, G. Jin et al., "A combined experimental and theoretical investigation of donor and acceptor interface in efficient aqueous-processed polymer/nanocrystal hybrid solar cells," *Science China Chemistry*, vol. 61, no. 4, pp. 437–443, 2018.
- [32] S. Lu, L. Sui, J. Liu et al., "Near-infrared photoluminescent polymer-carbon nanodots with two-photon fluorescence," *Advanced Materials*, vol. 29, no. 15, 2017.
- [33] B. Wang, J. Li, Z. Tang, B. Yang, and S. Lu, "Near-infrared emissive carbon dots with 33.96% emission in aqueous solution for cellular sensing and light-emitting diodes," *Science Bulletin*, vol. 64, no. 17, pp. 1285–1292, 2019.
- [34] J. Varshosaz, F. Hassanzadeh, H. Sadeghi, F. Firozian, and M. Mirian, "Effect of molecular weight and molar ratio of dextran on self-assembly of dextran stearate polymeric micelles as nanocarriers for etoposide," *Journal of Nanomaterials*, vol. 2012, Article ID 265657, 10 pages, 2012.
- [35] J. Varshosaz, F. Hassanzadeh, H. Sadeghi-Aliabadi, and F. Firozian, "Uptake of etoposide in CT-26 cells of colorectal cancer using folate targeted dextran stearate polymeric micelles," *BioMed Research International*, vol. 2014, Article ID 708593, 11 pages, 2014.
- [36] Y.-Z. Du, Q. Weng, H. Yuan, and F.-Q. Hu, "Synthesis and antitumor activity of stearate-g-dextran micelles for intracellular doxorubicin delivery," *ACS Nano*, vol. 4, no. 11, pp. 6894–6902, 2010.
- [37] P. Muley, S. Kumar, F. El Kourati, S. S. Kesharwani, and H. Tummala, "Hydrophobically modified inulin as an amphiphilic carbohydrate polymer for micellar delivery of paclitaxel for intravenous route," *International Journal of Pharmaceutics*, vol. 500, no. 1-2, pp. 32–41, 2016.
- [38] M. F. Rai and C. T. Pham, "Intra-articular drug delivery systems for joint diseases," *Current Opinion in Pharmacology*, vol. 40, pp. 67–73, 2018.
- [39] H. Tanzadehpanah, H. Mahaki, P. Samadi et al., "Anticancer activity, calf thymus DNA and human serum albumin binding properties of Farnesiferol C from *Ferula pseudalliacea*," *Journal of Biomolecular Structure and Dynamics*, vol. 37, no. 11, pp. 2789–2800, 2018.
- [40] N. H. Moghadam, S. Salehzadeh, H. Tanzadehpanah, M. Saidijam, J. Karimi, and S. Khazalpour, "In vitro cytotoxicity and DNA/HSA interaction study of triamterene using molecular modelling and multi-spectroscopic methods," *Journal of Biomolecular Structure and Dynamics*, vol. 37, no. 9, pp. 2242–2253, 2018.
- [41] C. S. Kumar, R. Ashok, S. L. Prabu, and K. Ruckmani, "Evaluation of betamethasone sodium phosphate loaded chitosan nanoparticles for anti-rheumatoid activity," *IET Nanobiotechnology*, vol. 12, no. 1, pp. 6–11, 2018.
- [42] M. A. A. Shafie and H. H. M. Fayek, "Formulation and evaluation of betamethasone sodium phosphate loaded nanoparticles for ophthalmic delivery," *Journal of Clinical & Experimental Ophthalmology*, vol. 4, no. 2, p. 2, 2013.
- [43] W.-S. Kim, J.-Y. Lee, B. Singh et al., "A new way of producing pediocin in *Pediococcus acidilactici* through intracellular stimulation by internalized inulin nanoparticles," *Scientific Reports*, vol. 8, no. 1, p. 5878, 2018.
- [44] D. Hou, R. Gui, S. Hu, Y. Huang, Z. Feng, and Q. Ping, "Preparation and characterization of novel drug-inserted-montmorillonite chitosan carriers for ocular drug delivery," *Advances in Nanoparticles*, vol. 4, no. 3, pp. 70–84, 2015.
- [45] Y. Wang, Z. Wu, Z. Ma et al., "Promotion of micelle stability-via cyclic hydrophilic moiety," *Polymer Chemistry*, vol. 9, no. 19, pp. 2569–2573, 2018.
- [46] D. Mandracchia, A. Trapani, T. Chlapanidas, G. Trapani, and G. Tripodo, "Enzyme controlled release of celecoxib from inulin based nanomicelles," *Journal of Cellular Biotechnology*, vol. 1, no. 1, pp. 107–118, 2015.